Analysis of the Causes of Variance in Resistance Measurements on Metal−Molecule−Metal Junctions Formed by Conducting-Probe Atomic Force Microscopy

Vincent B. Engelkes,[†] Jeremy M. Beebe,[‡] and C. Daniel Frisbie*[,†]

Department of Chemical Engineering and Materials Science and Department of Chemistry, University of Minnesota, Minneapolis, Minnesota 55455

Received: May 5, 2005; In Final Form: June 15, 2005

Alkanethiol tunnel junctions were studied using conducting-probe atomic force microscopy to determine causes of variability in measured resistance behavior. Measurements were made on Au/decanethiol/Au monolayer junctions, and effects of substrate roughness, tip chemistry, presence of solvent, extensive tip usage, applied load, and tip radius were examined. Resistance measurements yielded log-normal distributions under a variety of conditions, indicating that the origin of the variance is likely to be either changes in tunneling length or electronic overlap. Spreads in resistance values for a given tip were much less when flat, template-stripped Au substrates were used rather than rough, evaporated Au substrates. Chemical modification of tips with ethanethiol (C_2) or butanethiol (C_4) and performing measurements under cyclohexane were also found to reduce variance by a factor of about 2−4. Experiments performed with unmodified tips showed an increase in junction resistance over the course of hundreds of consecutive measurements, whereas junctions made with modified tips or under cyclohexane did not. Attempts to ascribe variance between tips to varying tip radii failed; however, decreases in resistance with increasing applied load on the tip contact were observed and could be interpreted in terms of conventional contact mechanics models.

Introduction

Many reports have been published on the current−voltage ($I-V$) characteristics of molecular tunnel junctions in which one or a small number of molecules are contacted by two metal electrodes.[1−33] Reported behavior is often consistent with nonresonant tunneling models, including temperature independence, exponential length dependence, and sigmoidally shaped $I-V$ traces. However, the precision of such measurements is often poor. For instance, in the authors' previous experiments with alkane monolayers, large variances have been observed in junction resistance measurements that were executed in a very similar fashion.[1,10,18,23,25] The accuracy, though not the precision, of the measurements has always been improved by relying on the statistics of many measurements. The causes of the large variances have not been explored extensively and may have interesting implications for correct interpretation of molecular conductance data.

This report covers a large number of resistance measurements on Au-substrate/decanethiol/Au-tip junctions made using conducting-probe atomic force microscopy (CP-AFM, see Figure 1). The goal is to better understand the sources of variance in these molecular conductance experiments and what controls are necessary to obtain better reproducibility in future work. Of primary significance to this report is the observation that measured resistance values appear to be distributed log-normally. That is, the variance stems from a parameter that affects the resistance exponentially. This is likely due to changes in the effective tunneling length or electronic overlap within the junction. Many parameters are considered as possible contributions to this variability including substrate roughness, tip chemistry, presence of solvent, extended tip usage, tip radius, and applied load.

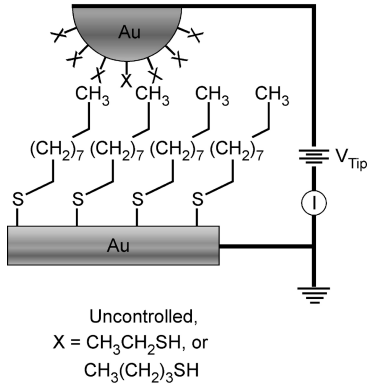

Figure 1. Schematic representation of a molecular tunnel junction formed using CP-AFM. A Au-coated AFM tip is brought into contact with a SAM of decanethiol on a Au-coated Si substrate. The tip is either unmodified, or modified with an ethanethiol (C_2) or butanethiol (C_4) monolayer. Voltage is swept at the tip and the resulting current is measured.

An essential issue is how to interpret the data statistically. For example, we are particularly interested in improving the precision of the measurements; therefore changes in variance (the square of the standard deviation) upon changing the experimental conditions are as important as the changes in the mean value (e.g., mean value of junction resistance). To compare both distribution means and variances we have used the bootstrap method. The bootstrap method is a convenient and computationally simple algorithm that can be used to estimate the standard error of any statistical parameter.[34,35] Algorithms used here were written in Igor Pro. In general, the method

* To whom correspondence should be addressed. E-mail: frisbie@cems.umn.edu.
[†] Department of Chemical Engineering and Materials Science.
[‡] Department of Chemistry.

10.1021/jp052348s CCC: $30.25
Published on Web 08/16/2005

involves randomly resampling an original data set. Each time the resampling is performed, the parameter of interest (mean, median, variance, skew, etc.) is determined from the resampled distribution and recorded. Many resamplings of the original data are done, resulting in a distribution of the parameter of interest. The standard error of the parameter can then be determined. The details of the method are described in the Results and Discussion section. With this method, we are able to compare quantitatively the differences in the precision of several measurements made under different experimental conditions. Such quantitative analysis of the experimental distributions is important because of the complex nature of conductance measurements on small numbers of molecules.

Experimental Section

Materials. Gold nuggets (99.999% pure) were purchased from Mowrey, Inc. (St. Paul, MN). Evaporation boats and chromium evaporation rods were purchased from R. D. Mathis (Long Beach, CA). Silicon (100) wafers were purchased from WaferNet (San Jose, CA). V-shaped AFM cantilevers and tips (model DNP) were obtained from Digital Instruments. Ethanol (reagent alcohol) and cyclohexane were purchased from Fisher Scientific. Decanethiol, ethanethiol, and butanethiol were obtained from Aldrich. EPO-TEK 377 epoxy was purchased from Epoxy Technology (Billerica, MA).

Sample and Tip Preparation. Silicon substrates and contact mode AFM tips were coated with metal using a Balzers thermal metal evaporator at a base pressure of $\sim 2 \times 10^{-6}$ Torr. Rough substrates and tips were coated with 1000 Å of Au at a rate of 1 Å/s after the deposition of a 50 Å Cr adhesion layer. Template-stripped flat substrates were made according to the recipe of Blackstock et al.[36] First, 5000 Å of Au was deposited onto a clean Si wafer. One square centimeter pieces of Si were then glued to this layer using epoxy, with the polished side to the Au surface. This sandwich structure was then baked at ~120 °C for 1 h or until cured. Substrates were pried away using a razor blade or tweezers, cleaving the Au/Si interface. Monolayers were self-assembled on both rough and flat surfaces by immersion in ~0.5 mM solutions of decanethiol in ethanol for at least a few hours. Some tips were also coated in monolayers by vapor deposition. This was done by enclosing the tip assemblies in a jar (attached to the inside of the lid) containing a solution of C_2 or C_4 in ethanol. Fresh batches of tips and monolayers were made after about four or five days.

Force Constant Determination. Cantilever force constants were determined by the thermal fluctuation method using an EG&G model 7260 lock-in amplifier.[37,38] The cantilever was mounted in the AFM, and the laser was aligned so that the power spectral density (PSD) could be directly measured from the deflection voltage on the AFM photodiode. The mean square deflection of the cantilever ($\langle z^2 \rangle$) due to thermal fluctuation was determined by integrating the first mode in the PSD (about 50−100 PSD traces were averaged together) followed by a division by 0.86 (it was assumed that 97% of the total power was partitioned into the first mode and that the photodiode measured an 89% demagnification of the deflection of this mode).[38] The force constant, k, was then determined from the following equation:

$$k = \frac{k_B T}{\langle z^2 \rangle} \tag{1}$$

where k_B is the Boltzmann constant and T is the temperature. This method ensures that when different cantilevers are used, the same load is applied for different experiments.

Standard *I*−*V* and Adhesion Measurements. Electrical junctions were formed by bringing a metallized tip into contact with a monolayer-coated substrate under 2 nN of applied load using a Digital Instruments MultiMode AFM in air (see Figure 1). Measurements under solvent were made with 12 nN of applied load to overcome the lack of adhesive forces, which were approximately 10 nN in air. During contact, voltage was swept at the tip using a Keithley 236 source/measure unit, and in general, 20 $I-V$ traces were recorded. Sets of $I-V$ traces obtained in this manner comprise what will be referred to as single measurements. Multiple measurements done at different locations on the sample surface were made for each tip. Thus, in a typical experiment, 20 traces were recorded per measurement, and multiple measurements (5−30) were made per tip. Resistance values were determined from the inverse of the slope of the $I-V$ data. Adhesive load was determined by the average of about five pull-off force measurements using the AFM control software (Nanoscope v.5). Measurements under cyclohexane were performed using a specially designed liquid cell for the MultiMode from Veeco Instruments Inc. Special drift experiments were also performed for comparison of rough and flat substrates as outlined below.

Comparison of Rough and Flat Substrates. Decanethiol films on rough and flat surfaces were compared by allowing the tip to drift across the surface while in contact. In these drift experiments, the tip was brought into contact with the decanethiol monolayer at a constant applied load of ~2 nN. The tip was then allowed to drift across the surface for about 5 min. A Keithley 6517 source/measure unit was used to apply a constant voltage of 0.05 V while monitoring junction current. The surface topography was simultaneously measured by monitoring the z-piezo voltage with a Keithley model 2000 electrometer directly from the signal access module of the AFM.

Tip Radii Measurements. Tip radii were determined by imaging a calibration grating of sharp spikes (TGT01) manufactured by MikroMasch with a conical angle less than 20° and a radius of curvature less than 10 nm. A few images were gathered at a scan size of 300 nm and a rate of 1.81 μm/s. Trace and retrace height images were very comparable, indicating that this rate of imaging was not too high. Eight sections were taken at various angles around the apex of each image. The corresponding sections from each image were averaged together, and the average section was fit with a fourth-degree polynomial over 20 nm centered on the apex of the tip. The curvature at each angle was determined by the second derivative of the curve-fit, evaluated at the apex. The effective tip radius was defined by a geometric average of these radii, equivalent to defining the effective radius of the irregular ellipse as the radius of the circle having the same area.

Resistance versus Load Measurements. Junction resistance and applied load were measured simultaneously while the tip was cycled slowly (20 nm/s) through a force−distance curve using the AFM control software (Nanoscope v.5). The software raised the AFM piezo element toward the tip until the tip and substrate were in contact and a set level of cantilever deflection was achieved (~500 nm). The software then reversed the piezo motion, reducing deflection and separating the tip and substrate from contact. The tip was held at a constant potential of 0.2 V and junction current measured using a Keithley 6517 source/measure unit. The cantilever deflection was recorded using a Keithley 2000 electrometer connected directly to the photodiode voltage output. For the MultiMode, this was the "ln0" BNC

connection on the signal access module. Multiple traces of this nature were recorded and averaged together by binning the data over small load intervals.

Results and Discussion

Statistical Analysis. When statistical parameters are reported in this paper, they are a result of geometric averaging. Resistance values (R_i) obtained in these experiments appear to originate from log-normal distributions, i.e., the logarithms of the resistance values appear to be distributed according to a normal bell curve. For this reason, the average and variance values are obtained from the sample set of $\ln(R_i)$. Plots of resistance versus the independent variable (e.g. radius, load, etc.) on logarithmic axes show symmetric error bars. When distribution variances (*Var*) are quoted, they are of the log-normal distribution and are unitless:

$$Var(\ln(R)) = \frac{\sum_{i=1}^{n}(\ln(R_i) - \langle \ln(R) \rangle)^2}{n-1} \tag{2a}$$

$$\langle \ln(R) \rangle = \frac{\sum_{i=1}^{n} \ln(R_i)}{n} \tag{2b}$$

where R_i is a single resistance observation, and n is the number of observations of the distribution. *Var* is referred to as the log-normal variance. Equation 2b represents the mean value of the log-normal distribution. Hypothesis tests for the comparison of various distribution means and variances are performed using the quantities of eq 2, although when resistance values are stated they are converted to units of resistance by exponentiation of eq 2b.

Hypothesis tests are used to determine the degree of certainty in the difference between statistical parameters from two different samples. In this paper, means and variances of resistance measurements are compared for molecular junctions under different experimental conditions. The problem we face is to somehow *quantify* whether the means and variances of two separate sets of resistance measurements (taken in air and under solvent for example) are different. To make meaningful comparisons, knowledge of the standard errors in the sample mean and variance is needed (i.e., the certainty that the sample parameter is close to the true population parameter). Determination of the standard error in a sample mean (SE_{mean}) is defined simply by the following equation involving sample variance:

$$SE_{mean} = \left(\frac{Var}{n}\right)^{1/2} \tag{3}$$

However, the *standard error of the variance* is not so easily acquired, and comparison of sample variances requires a different approach. In this paper, we have chosen to use the bootstrap method for estimation of standard errors[34,35] and, for consistency, we have applied the technique to sample means as well as sample variances.

The bootstrap method for estimation of standard errors is described as follows: The sample set of $\ln(R_i)$ values for a given set of data is resampled by randomly choosing n values from the sample set, where n is the number of samples in the original set. The mean and variance of this new, resampled set are then determined and referred to as bootstrap replications of the sample mean and variance. This process is repeated 10^5 times on the original data set, resulting in 10^5 bootstrap replications of the mean and variance for the sample. From this bootstrapped distribution, confidence limits on the true population mean and variance can be determined. For example, we can quote a range of values that we are 95% confident bounds the population mean or variance. The large number of resamplings (10^5) contains many duplicate replications because there are not 10^5 unique resamplings obtainable from the original sample set (the original sets contain ~10−30 observations). Therefore, the calculations are convergent once ~500 resamplings have been performed. However, smoother histograms result from much larger resampling numbers, which are not particularly time-consuming to generate. As with any statistical technique, the primary limitation is the assumption that the sample is a good estimate of the population distribution.

To quantify the confidence that a difference exists between pairs of statistical parameters, a series of hypothesis tests are performed. The hypothesis tests begin with a null hypothesis in which the two parameters are assumed to be equal, and proceed by attempting to invalidate this assumption in favor of an alternative hypothesis (i.e., that one parameter is greater or less than the other). Comparison between mean values is done by defining the following null hypothesis:

$$\langle \ln(R^x) \rangle - \langle \ln(R^y) \rangle = 0 \tag{4}$$

where the superscripts x and y refer to the two samples being compared. The mean test statistic, $Z^{x,y}_{mean}$, is then defined as

$$Z^{x,y}_{mean} \equiv \langle \ln(R^x) \rangle - \langle \ln(R^y) \rangle \tag{5}$$

Rejection of the null hypothesis, i.e., determination that the means are not equal, can be done if $Z^{x,y}_{mean}$ is significantly different than zero. A bootstrap replication of the mean is generated for each of the two samples (x and y) being compared. The difference of these two replicated means is then the bootstrap replication of $Z^{x,y}_{mean}$.

Comparison between variance values is done by defining a slightly different null hypothesis:

$$\frac{Var(\ln(R^x))}{Var(\ln(R^y))} = 1 \tag{6}$$

The variance test statistic, $Z^{x,y}_{var}$, is then defined as

$$Z^{x,y}_{var} \equiv \frac{Var(\ln(R^x))}{Var(\ln(R^y))} \tag{7}$$

Ratios are preferred for variance comparison because the variance is not a normally distributed parameter, whereas the mean is normal. Therefore, eq 7 appears more normal than if the difference of variances were calculated. Rejection of the null hypothesis, i.e., determination that the variances are not equal, can be done if $Z^{x,y}_{var}$ is significantly different than unity. $Z^{x,y}_{var}$ is determined in a manner similar to that used for $Z^{x,y}_{mean}$, except that bootstrap replications of the variance are obtained and their quotients determined.

The bootstrapped replications of $Z^{x,y}_{mean}$ and $Z^{x,y}_{var}$ are plotted as histograms (counts versus Z), which when normalized by the total number of counts represent the probability distribution of Z values. From this distribution a confidence interval of Z can be defined. If the condition for a true null hypothesis (i.e. $Z^{x,y}_{mean} = 0$) lies outside this interval, then the null hypothesis can be rejected. In other words, rejection of the null hypothesis indicates

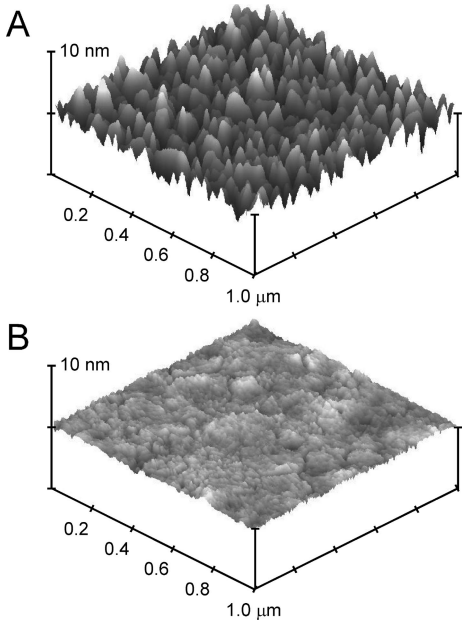

Figure 2. AFM topographical images of rough, thermally evaporated (A) and flat, template-stripped (B) Au substrates. RMS roughness values of substrates over 1 μm^2 are 13.3 and 2.8 Å respectively.

that the two distributions being tested are statistically different. The area of the rejection region outside of the confidence interval is referred to as the significance level of the test, α. The smallest level of significance (area) for which the null hypothesis can be rejected is defined as the *p*-value and is convenient for quantifying the probability of rejecting a true null hypothesis. Smaller *p*-values indicate a higher certainty that the null hypothesis should be rejected in favor of the alternative hypothesis. That is, smaller *p*-values represent larger statistical certainty that the two distributions being compared are different. This *p*-value can be obtained from the cumulative probability (integral of the probability distribution) evaluated at $Z^{x,y}_{mean} = 0$ or $Z^{x,y}_{var} = 1$.

***I*−*V* and Drift Measurements on Rough and Flat Substrates.** Prior to monolayer formation, flat and rough substrates were imaged in tapping mode to demonstrate the topographical differences between the two. In agreement with Blackstock et al.,[36] template-stripped substrates have a significantly lower RMS roughness value of 2.8 Å compared to 13.3 Å for rough surfaces over an area of 1 μm^2 (see Figure 2). The RMS roughness of the templated substrates falls below 1 Å for scan sizes smaller than 1000 nm^2. Considering the size of the contact area in CP-AFM junctions (estimated to be ~50 nm^2), these substrates can be considered atomically flat. The effect of the surface roughness on conductance reproducibility is shown in Figures 3 and 4. Comparison between 100 *I*−*V* traces taken on rough (Figure 3A) and flat substrates (Figure 3B) indicates that the variance between traces is much lower when surface topography is minimized. For the data in Figure 3, there is 95% probability that the log-normal variances ($Var(\ln(R))$) are between 0.9−2.1 and 0.3−0.5 for measurements taken on rough and flat Au substrates, respectively. These values indicate that there is little chance that the two distribution variances are the same. In fact, the *p*-value (probability that the distributions have the same variance) is less than 0.001.

Figure 4 illustrates a possible explanation for the difference in variance on rough and smooth Au. During measurements, the AFM piezo is susceptible to thermal drift such that the tip position does not remain constant over the surface. As the

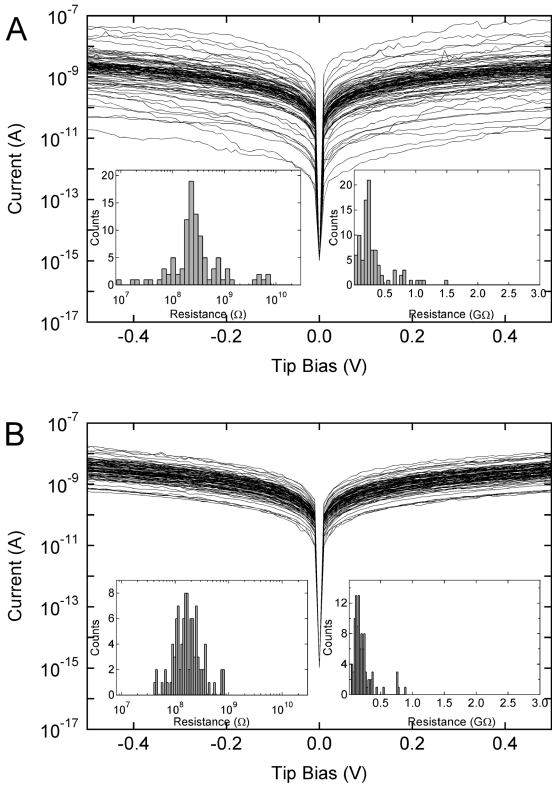

Figure 3. (A) 100 *I*−*V* traces obtained using a single representative AFM tip on rough thermally evaporated Au substrates. (B) 100 *I*−*V* traces obtained with a single representative AFM tip on flat template-stripped Au substrates. Trace-to-trace variance is significantly decreased when flat Au substrates are used. Data in panels A and B are not collected with the same tip. Insets show the histograms of junction resistances calculated over ±0.5 V on log (left) and linear (right) axes. Distributions appear normal on log axes and are therefore concluded to be log-normal.

surface drifts beneath the tip, considerably more topography is encountered in the case of rough substrates than in the case of flat substrates. This can be seen in comparison of the dotted lines in Figure 4. In Figure 4A (rough substrate), there is more change in height during a drift period of 5 min than in Figure 4B (flat substrate). This topography is accompanied by varying resistance (solid lines). There is not a clear one-to-one correspondence between the height and resistance for the rough substrate; however, the resistance varies over orders of magnitude, particularly where the height changes quickly. Another interesting observation that can be made from Figure 4 is that the resistance measured on the flat substrate is greater than that measured on the rough substrate. This conclusion cannot be drawn in Figure 3, because data in panels A and B of Figure 3 are not taken with the same tip. One explanation for this phenomenon is that a larger contact area is probably present in the case of rough substrates as the tip slides between the Au grains in the substrate.

The fact that the resistance varies over orders of magnitude and appears to be distributed log-normally indicates that the variance stems from a parameter that affects the resistance exponentially. Therefore, it is very unlikely that changes in contact area alone are responsible for the observed variance, as this would weakly affect the resistance. The variation is probably due to effective changes in the tunneling length, as the resistance is known to depend exponentially on the length of the junction.[13,17,18,21,29] The variance could be attributed to molecules being contacted in places other than the terminal methyl group further down the chain of the molecule. This is a more probable

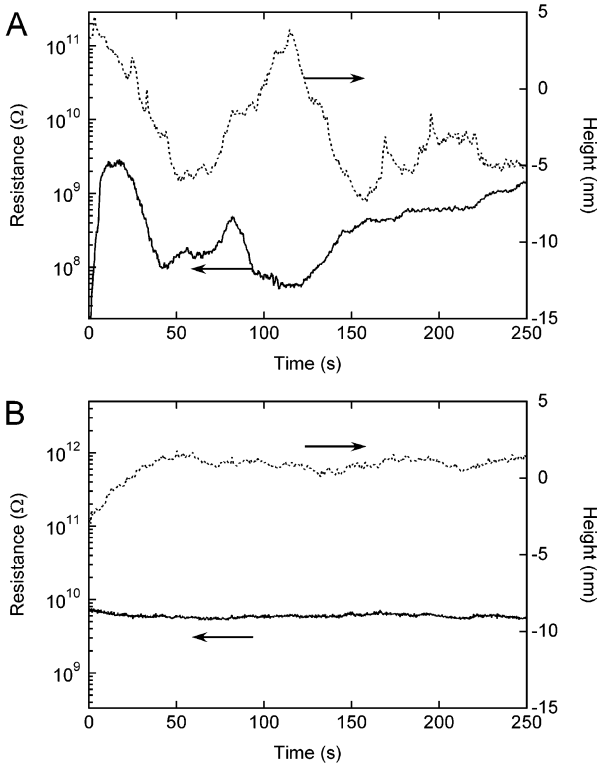

Figure 4. Resistance (solid lines) and height (dashed lines) measured simultaneously while the AFM tip is under normal force feedback and as it drifts over the decanethiol monolayer in air. Data for both rough (A) and flat (B) substrates are displayed and are taken with the same tip. Larger variances in measured resistance and height are apparent for the rough substrates, with some correlation. Y-axes in (B) are scaled to have the same percent range as in (A).

event on the rough substrate, where the monolayer film is likely more disordered, causing it to appear thinner on average. The increased disorder is also consistent with the reduced resistance observed on rough substrates. A final contribution to the larger resistance variance on rough substrates is the presence of a greater degree of torsional forces. Although the AFM is able to control the deflection of the cantilever perpendicular to the surface, thereby controlling the applied normal load, there is no control over the lateral forces that are present as the tip drifts over a rough surface. These forces could potentially induce conformational changes in the monolayer and increase the effective pressure in the junction. Such factors could affect the resistance to a higher degree (i.e., exponentially) than changes in contact area. Nonetheless, there clearly exists a better controlled contact between the monolayer and tip when flat substrates are used. For this reason, the rest of this report discusses only experiments performed on flat substrates.

Variance of Resistances Obtained with Different Tips. The previous section described how $I-V$ traces measured on flat substrates have much less variance than those made on rough substrates. This is a large step forward in attempting to understand the details that govern conductance in CP-AFM junctions, particularly in terms of the tip/monolayer contact. However, when comparing the resistance measured by many different tips, more questions arise. Figure 5 shows the large variance in resistance between experiments performed with different AFM tips. The spread in resistance values measured with 32 different tips, i.e., the tip-to-tip variance, was over 4 orders of magnitude, whereas the spread in resistance values measured with a single tip, i.e., the trace-to-trace variance, was approximately 1 order of magnitude (Figure 3B). The 95%

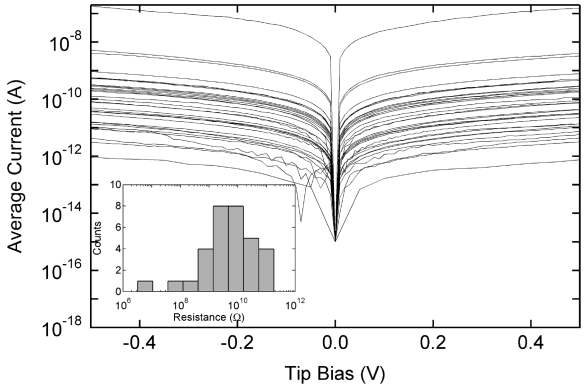

Figure 5. Average $I-V$ data of Au/decanethiol/Au junctions for 32 different tips in air. Each of the lines is an average of about 50 $I-V$ traces. Comparison to Figure 3 illustrates the difference in magnitude between tip-to-tip variance and trace-to-trace variance. Inset shows the log-normal distribution of junction resistances calculated over ±0.5 V.

confidence interval of the log-normal tip-to-tip variance for the data displayed in Figure 5 is equal to 5 ± 3. Comparison of this variance and the trace-to-trace variance (0.4 ± 0.1) yields a p-value that is again less than 0.001. This suggests that, although the tip/monolayer contact is rather consistent throughout an experiment with a single tip, there is a significant difference between tip/monolayer contacts when different tips are involved.

There may be many reasons for this: (1) Different tips have different levels of contamination, resulting in varying thicknesses of the tunnel gap or electronic structure of the tip. (2) Atmospheric humidity is different during each experiment, resulting in varying water layers at the tip/monolayer interface. (3) Each tip has a different radius of curvature, resulting in a different contact area and a different pressure and junction stress at the same applied load. As in the previous section, all resistance distributions appear to be log-normal; therefore, it is likely that points (1) and (2) are dominant factors contributing to the variance.

Modification of Tips with Short-Chain Alkanethiol Monolayers. Sensitivity of junction resistance to tip contamination was tested by performing experiments where sets of tips were chemically modified by the formation of either C_2 or C_4 monolayers. The results of experiments performed with chemically modified tips were then compared to those obtained with unmodified tips in hopes of demonstrating a reduction or control of the level of contamination. Figure 6 is a plot of average junction resistance versus the length of the monolayer adsorbed to the tip. The error bars in Figure 6 represent one standard deviation of the resistances. It is important to consider that, although the unmodified tip resistances are placed along the abscissa at zero length of adsorbate, it is possible that contaminants are present. Contaminants may also be present in the cases of modified tips.

Two observations can be made from Figure 6. First, there is less tip-to-tip variance when modified tips are used, and modification with C_4 is more effective at reducing this variance than C_2. This suggests that contamination of the tip is indeed a significant problem, contributing to variance in measurements made between different tips, and that use of monolayers for modification of tips successfully removes some or all of the contaminant. Second, the average resistance of junctions made with C_2-modified tips is surprisingly *lower* than the average resistance of junctions made with unmodified tips. This is not an expected result because presumably the junction becomes

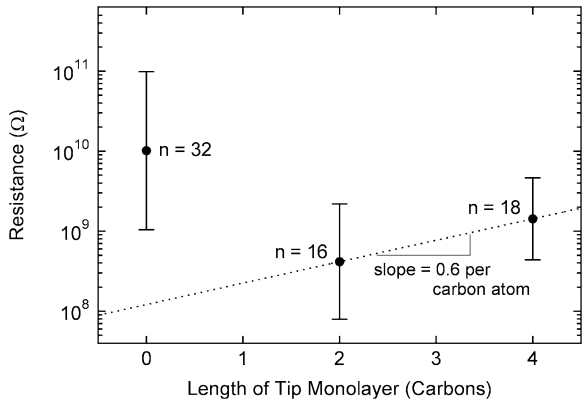

Figure 6. Measured resistance values for Au/decanethiol/Au junctions in air, where the tip electrode is either unmodified or modified with C_2 or C_4. Each data point represents the geometrically averaged resistance for n different tips. The slope between modified tips is similar to the value of β accepted for alkane systems.

TABLE 1: List of Tip-to-Tip and Average Trace-to-Trace Log-Normal Resistance Variances for Experiments Performed under Different Conditions[a]

conditions	trials	tip-to-tip log-normal variance	trace-to-trace log-normal variance
unmodified (air)	32	5 ± 2	0.31 ± 0.05
C_2-modified (air)	16	2.8 ± 0.8	0.40 ± 0.09
C_4-modified (air)	18	1.4 ± 0.5	0.33 ± 0.07
unmodified (C_6H_{12})	8	1.6 ± 0.7	0.5 ± 0.1

[a] Error values are one standard error.

approximately 20% thicker with the introduction of a C_2 film on the tip. C_4-modified tips also produce junctions with lower resistance than unmodified tips, though the effect is less pronounced. The observation of lower junction resistance upon chemical modification of the tip can be explained by either one of two theories or a combination thereof: (1) either the level of contamination is very large when tips are left unmodified, such that the thickness of the contaminant is greater than a C_4 monolayer, (2) the unmodified tips are contaminated with residual physisorbed decanethiol molecules from the substrate, or (3) the chemisorption of the monolayer to the Au tip reduces the barrier to electronic transport enough to offset the increase in junction thickness.

The trend of junction resistances with C_2- and C_4-modified tips suggests that the thicknesses of these junctions scale as expected, i.e., the slope of the line between the two averages is 0.6 per carbon atom, somewhat less than, though reasonably near, the accepted value of the tunneling decay parameter, β, for alkane systems (1.1 per carbon atom).[1,9,10,12,22,23,27] The facts that this measured slope is less than 1.1 per carbon atom and that the variance of junction resistances composed of C_2-modified tips is slightly larger than for C_4-modified tips could be evidence that C_2 is less effective at reducing contaminants from the tip surface. A subtle effect to consider is dependence of trace-to-trace variance on tip modification. Table 1 lists the tip-to-tip variances and average trace-to-trace variances observed for each set of tips under each different experimental condition (e.g. tip modification). No significant difference in the trace-to-trace variances was observed upon tip modification; however, differences in tip-to-tip variances were very pronounced.

Confidence in Tip-to-Tip Statistics of Chemically Modified Tip Junctions. In the previous section, it was concluded that modification of AFM tips by deposition of C_2 and C_4 monolayers resulted in a decrease in both junction resistance and the variance of the resistance. Histograms of bootstrap replications of mean junction resistance and resistance variance for each type of tip modification (unmodified, C_2-modified, and C_4-modified) are displayed in Figure 7. It is important to note that these histograms are not raw data, but are generated from the raw data using the above-described bootstrap technique for determining standard error in statistical parameters. The widths of the histograms represent the confidence in the corresponding parameter, and the shapes are smooth and regular, indicating that an adequate amount of data has been obtained for statistical analysis. Figure 7 qualitatively illustrates that the reduction of junction resistance with tip modification can be accepted with a high degree of confidence (the histograms do not overlap much at all), and that the reduction in variance can also be accepted, although with slightly less confidence (more overlap of histograms is observed).

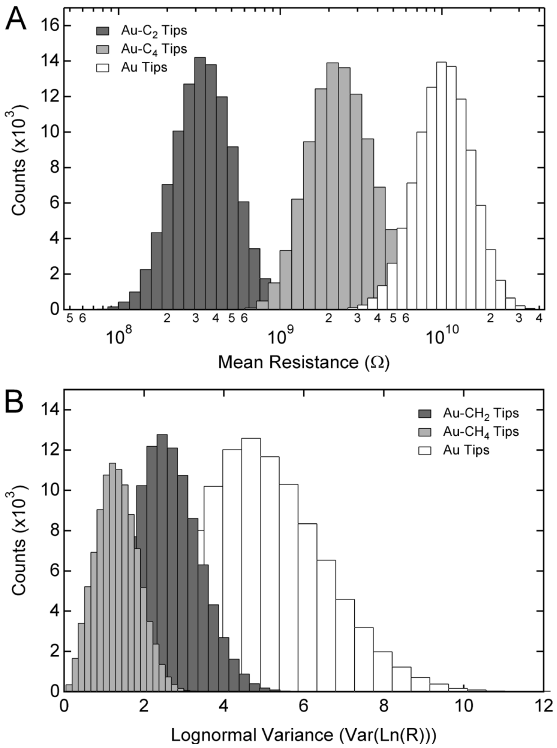

Figure 7. Distributions of mean resistance (A) and variance (B) for Au/decanethiol/Au junctions in air. Tip electrodes are either unmodified (white), modified with C_2 (dark gray), or modified with C_4 (light gray). Histograms were generated by resampling the sample distribution, resulting in bootstrap replications of the sample means and variances. 10^5 bootstrap replications were performed.

Figure 8A is a histogram of 10^5 bootstrap replications of $Z^{x,y}_{\text{mean}}$ (eq 4), where x and y are unmodified and C_2-modified tips, respectively. The cumulative probability is also displayed as determined by the integral of $Z^{x,y}_{\text{mean}}$. The probability of falsely concluding that the means are different (the p-value) is given by the value of the cumulative probability evaluated at $Z^{x,y}_{\text{mean}} = 0$, which in this case is very small ($p < 0.001$). Hence, there is nearly a 100% chance that the mean value of the junction resistance for unmodified tips is different than that for C_2-modified tips. Table 2 lists the p-values associated with rejection of the null hypotheses of the sample means and the ratio of measured resistances for each comparison. The low p-values in Table 2 indicate that the differences between the three mean resistance values in air are clearly statistically significant. Figure 8B is a histogram of 10^5 bootstrap replications of $Z^{x,y}_{\text{var}}$ (eq 6) and its cumulative probability, where x and y are

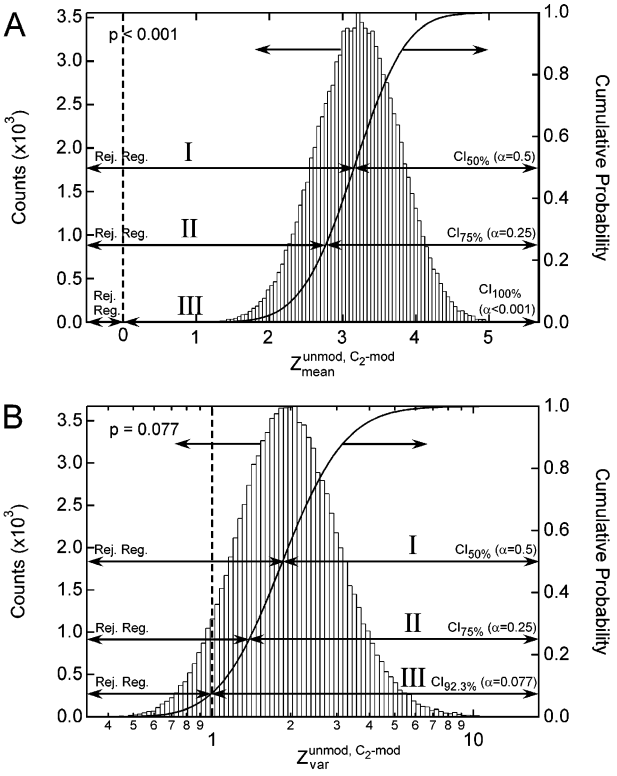

Figure 8. Examples of test statistic distributions for comparison of sample means (A) and sample variances (B) for experiments performed with unmodified and C_2-modified tips. The test statistic for comparing the sample means (eq 5) was generated by the difference of the bootstrap-replicated means for the two samples. The test statistic for comparing the sample variances (eq 7) was generated by the ratio of the bootstrap-replicated variances for the two samples. 10^5 bootstrap replications were performed in each case. Rejection of the null hypothesis involving the sample means is possible when the distribution of Z_{mean} is significantly far from zero. Rejection of the null hypothesis involving the sample variances is possible when the distribution of Z_{var} is significantly far from unity. I, II, III in each panel show three confidence intervals (CIs) and rejection regions with α equal to 0.5, 0.25, and less than 0.001 (A) or 0.077 (B), respectively. In each case, the null hypothesis ($Z_{mean} = 0$ or $Z_{var} = 1$, represented by the dashed vertical lines) is within the rejection regions. The *p*-value is the smallest value for α where the null hypothesis is found within the rejection region (e.g. if α were equal to 0.076, $Z_{var} = 1$ would be within the CI and not the rejection region).

TABLE 2: Comparison of Resistance Mean Values[a]

comparison		mean ratio ($\exp(Z^{x,y}_{mean})$)	
x	*y*	R_x/R_y	*p*-value
unmodified (air)	C_2-modified (air)	24	<0.001
unmodified (air)	C_4-modified (air)	7.1	<0.001
unmodified (air)	unmodified (C_6H_{12})	8.9	<0.001
C_2-modified (air)	C_4-modified (air)	0.29	0.004
C_2-modified (air)	unmodified (C_6H_{12})	0.37	0.032
C_4-modified (air)	unmodified (C_6H_{12})	1.3	0.358

[a] The mean ratio is the quotient of the two (*x* and *y*) compared resistance means. P-values indicate the probability of rejection of a true null hypothesis (i.e., the probability that the compared resistance means are actually equal).

unmodified and C_2-modified tips, respectively. The *p*-value in this case is given by the value of the cumulative probability evaluated at $Z^{unmod,C2-mod}_{var} = 1$. Table 3 lists the *p*-values for the sample variances and the ratio of the log-normal variances for each comparison. The *p*-values in Table 3 indicate that the reduction in sample variance for measurements performed in

TABLE 3: Comparison of Log-Normal Resistance Variance Values[a]

comparison		variance ratio ($Z^{x,y}_{var}$) var(ln(R_x))/	
x	*y*	var(ln(R_y))	*p*-value
unmodified (air)	C_2-modified (air)	1.9	0.077
unmodified (air)	C_4-modified (air)	3.7	0.002
unmodified (air)	unmodified (C_6H_{12})	3.2	0.007
C_4-modified (air)	C_2-modified (air)	2.0	0.110
C_2-modified (air)	unmodified (C_6H_{12})	1.7	0.163
C_4-modified (air)	unmodified (C_6H_{12})	0.86	0.394

[a] The variance ratio is the quotient of the two (*x* and *y*) compared log-normal resistance variances. P-values indicate the probability of rejection of a true null hypothesis (i.e., the probability that the compared resistance variances are equal).

air with modified tips is statistically significant. For example, the reduction of variance by a factor of 3.7 with C_4-modification has a *p*-value of 0.002. In other words, we are 99.8% confident that the variance change associated with C_4-modification is real. The reduction of variance by a factor of 1.9 with C_2-modification has a *p*-value of 0.077. The difference between variances of C_2-modified and C_4-modified tips is less significant, although the confidence in the difference is still 89.0%.

Resistance Measurements Made under Cyclohexane. To address further the issue of tip contamination, particularly as a result from atmospheric humidity, a series of measurements were made under cyclohexane. The adhesive force observed under cyclohexane was negligibly small and not recorded. *I*−*V* measurements made with 2 nN of applied load were very resistive and irregular in comparison to those measurements made in air. Measurements improved substantially when the applied load was increased to 12 nN in order to compensate for the lack of adhesive load present in air (~10 nN). If Derjaguin−Muller−Toporov (DMT) contact mechanics are applicable to these junctions, as suggested by other research,[39,40] 12 nN of applied load under cyclohexane results in junction loads similar to those obtained with 2 nN of applied load in air.

Figure 9 is a histogram of 10^5 bootstrap replications of resistance means and variances for unmodified tips in air and under cyclohexane. The smoothness of the histograms in Figure 9 suggests that the sample size is adequate. Both resistance and tip-to-tip variance decrease significantly for unmodified tips upon immersion of the junctions in cyclohexane. The *p*-values associated with comparison of the mean resistances and variances are 0.001, and 0.006, respectively. Thus, the measurements under cyclohexane versus those in air are clearly different, and significantly, the mean and variance in resistance under cyclohexane is much smaller. We postulate that the large tip-to-tip variance in the ambient junctions is attributable to an uncontrollably thick contaminant layer or water layer that is present in the ambient experiments. Variability in the thickness of this contaminant layer on different tips could lead to log-normal variance in measured tip-to-tip variance of resistance. Immersion of the junctions in cyclohexane offers a more controlled solvent layer at the tip/monolayer interface. The fact that the resistance decreases upon immersion suggests that the solvent layer formed is thinner than the average contaminant layer in ambient conditions. These findings are in agreement with what is observed upon chemical modification of the tips. Introduction of an aliphatic monolayer to the tip cleans the surface of contaminants and also increases the hydrophobicity of the tip, thereby possibly reducing formation of water layers and reducing the tip-to-tip variance of resistance.

Junctions formed using unmodified tips in cyclohexane exhibit behavior similar to the behavior exhibited by those

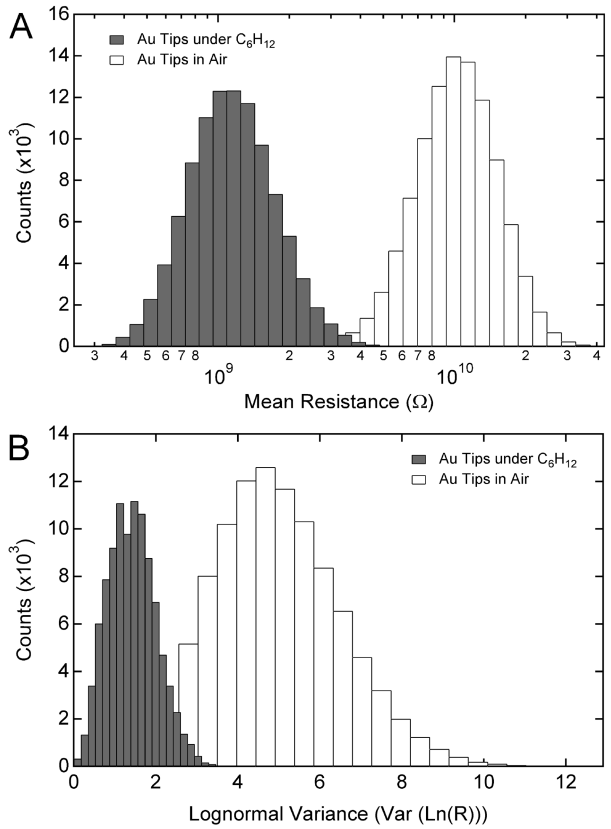

Figure 9. Distributions of mean resistance (A) and variance (B) for Au/decanethiol/Au junctions in air under 2 nN of applied load (white) and under cyclohexane under 12 nN of applied load (dark gray). Tip electrodes are unmodified. Histograms were generated by resampling the sample distribution, resulting in bootstrap replications of the sample means and variances. 10^5 bootstrap replications were performed.

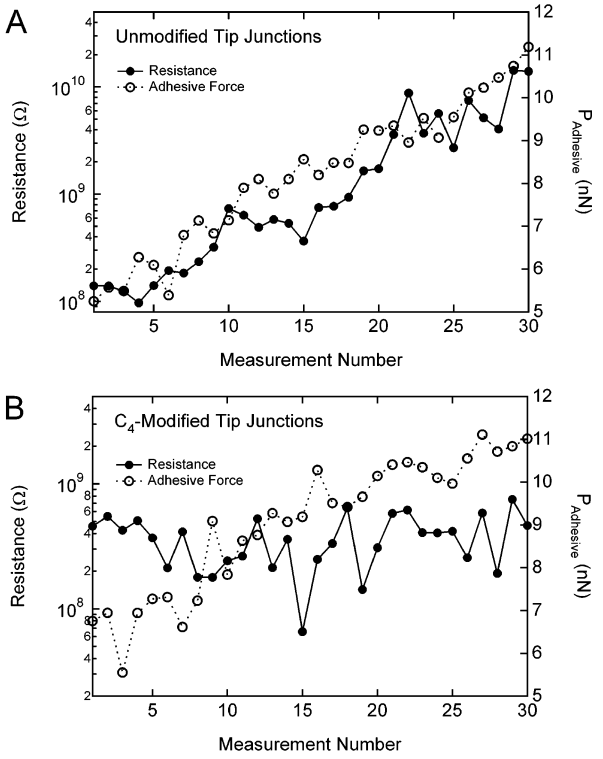

Figure 10. Junction resistance and adhesive force for consecutive measurements of Au/decanethiol/Au junctions collected in different locations on the same sample in air. Each resistance data point is the average of the resistances of 20 $I-V$ traces (600 individual $I-V$ traces are present per panel). Data in panel A are collected with a representative unmodified tip and data in panel B are collected with a representative C_4-modified tip. In each case, adhesive force is observed to increase with consecutive measurement. However, resistance is observed to increase for the unmodified tip junction and remain essentially constant for the C_4-modified tip junction with consecutive measurement.

formed using C_4-modified tips in the ambient air. In both cases, the tip-to-tip variances and mean resistances are statistically similar (*p*-values for comparison of resistance means and variances are 0.36 and 0.39, respectively) and lower in comparison to the ambient, unmodified tip resistances. Similarity might suggest that immersion in cyclohexane and tip modification address the same root cause of imprecision (e.g., a water layer) in unmodified tip experiments. The similarity of the mean values implies that the solvent layer is either a monolayer of upright cyclohexane molecules or a stack of a couple layers of molecules, having a thickness similar to that of a butanethiol monolayer. It should also be considered that immersing the monolayers in cyclohexane may change the conformation of the molecular tails and affect the conductivity.

Extensive Usage of Tips. A series of many measurements (20−30) at different locations on the substrate, each comprised of 20 $I-V$ traces, were carried out with individual tips to determine the dependence of junction resistance on the number of times the surface was contacted. Such dependence could be indicative of a change in the level of tip contamination when tips are used for an extensive period of time. Figure 10A illustrates this effect for a representative unmodified Au tip. Resistance increases with consecutive measurement (i.e., number of times the tip engages the surface), as does the adhesive force. The monotonic increase of resistance suggests that the tip indeed becomes more contaminated as it is used, presumably with free decanethiol molecules or by removal of decanethiol molecules bound to the substrate. The increase in adhesive force is not consistent with this, because contaminated Au has lower surface energy than bare Au[39,41] and should result in lower adhesive forces. While the tip probably does not begin in a pristine state, the level of contamination may be lower prior to the tip being contacted to the monolayer many times. It is also likely that the tip is plastically deformed and blunted during the experiment, thereby increasing the contact area. These effects would alter the resistance in opposite ways, but the effect of the contamination would be greater in magnitude because tunneling resistance scales exponentially with junction thickness. It should be stressed that although contamination is observed to increase over a large number of measurements, the CP-AFM technique still provides a good method by which to measure junction resistance if care is taken to reduce the number of times the tip is contacted to the surface. For instance, previously reported measurements by our group[1,10,18,23,25] and the prior experiments described in this work were obtained by engaging the surface only about five times.

Figure 10B shows the change in resistance and adhesive force over a set of 30 measurements, each comprised of 20 $I-V$ traces, obtained with a representative C_4-modified tip. As in Figure 10A, the adhesion is observed to increase with consecutive measurement; however, the resistance is observed not to trend with the measurement number. Decreases in junction resistance are observed for junctions with C_2-modified tips and for unmodified tip junctions under cyclohexane. The hypothesis that the tips become blunt as many measurements are made and contact area increases is consistent with the increase in adhesive force. No trend in resistance would be anticipated because it would be difficult for free thiol molecules to bond to an already

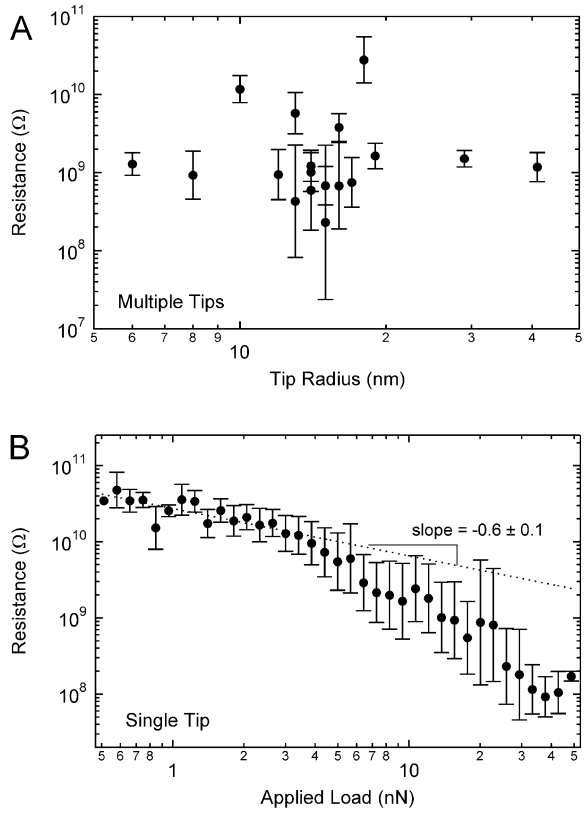

Figure 11. Junction resistances of C_4-modified tips versus tip radius in air (A). Correlation of resistance and tip radius is not observed. Resistance versus applied load for unmodified tips under cyclohexane (B). Junction resistance is observed to decrease with increasing applied load according to eq 7. The slope of the line is determined at low applied loads between 0.5 and 5.0 nN, prior to onset of clear deviation from this slope.

modified tip and contamination would not occur. The effect of a slightly increased contact area on the resistance would not be strong and, in fact, was not observed in the case of C_4-modified tips. In the case of unmodified tips under cyclohexane, contamination of the tip may be reduced over time due to a cleaning action of the solvent. In the C_2-modified tip junctions, the disordered short-chain film on the tip is likely to be susceptible to degradation, resulting in a reduction of junction thickness over time. This degradation may be less likely in the case of C_4-modification, as the film is slightly thicker and more ordered. These factors would have a much stronger effect on the junction resistance than an increase in contact area.

Contact Area Dependence of Junction Resistance. Resistances of C_4-modified tip junctions are plotted versus measured tip radius in Figure 11A. It would be expected that larger tips should provide larger contact areas (A) according to the following power-law relation:

$$A = \pi\left(\frac{3P_{\text{eff}}}{4E^*}r\right)^{2/3} \tag{8}$$

where r is the tip radius, E^* is the effective modulus, and P_{eff} is a combination of the applied load and adhesive load.[39] According to DMT contact mechanics this combination is simply the sum of the two loads.[39,42] If the resistance is assumed to scale inversely with the contact area, the power-law scaling in Figure 11A should be about $-{}^2/_3$. This is not observed; however, the expected trend is very weak, and contamination has been demonstrated to have a large effect on the junction resistance. It is also likely that tiny asperities and variations in the quality of conductivity at the very end of the tip exist, adding a significant amount of variance to these measurements. Therefore, it is not surprising that we do not have sensitivity to this dependence.

Figure 11B is a plot of resistance versus applied load for a single unmodified tip under cyclohexane. This particular experiment was chosen because it eliminates the problem of adhesive forces, i.e., the effective load is simply the applied load. The power-law fit performed over the low-load regime, prior to the noticeable deviation from linearity, exhibits a slope of -0.6 ± 0.1, in agreement with eq 8. The increased steepness of the slope with increasing load indicates that more than just an increase in contact area must be considered at large loads. Nonetheless, this result validates the use of conventional contact mechanics for analysis of CP-AFM junctions. It shows that a dependence of resistance on contact area can be established if tip-to-tip variance is eliminated, for instance, when only one tip is considered and the load is varied. The fact that we are not sensitive to the dependence of junction resistance on tip radius when different tips are used is due to a tip-to-tip variance that is too large and predominantly controlled by other factors, such as contamination.

Conclusions

Au/decanethiol/Au tunnel junctions have been studied extensively using CP-AFM in order to address issues of reproducibility. Our data indicate large variances are observed in junction resistance measurements, which can be reduced by controlling important parameters including substrate roughness, tip chemistry, presence of solvent, and extensive tip usage. Previous reports by us and others have addressed reproducibility by making large numbers of measurements in order to get reliable statistics. While that approach is clearly valid, a quantitative assessment of experimental precision as described here is necessary to devise strategies for improving the measurement.

It has been demonstrated that substrate roughness greatly affects the resistance of such junctions by introducing a large variance in the measured resistance, and by reducing the magnitude of the resistance. Trace-to-trace variances for given tips where natural drift (due to the piezo-scanner) of the monolayer surface beneath the tip was observed provide evidence for this. The distribution of measured resistances appears to be log-normal and, therefore, is likely the result of a variation in effective tunneling length. We conclude that flatter surfaces create a more stable tip/monolayer interaction by reducing random changes in contact area and lateral compression, and they provide a thicker and more uniform monolayer as observed in the reduction of variance and increase in mean resistance.

Resistance measurements made with different tips yield log-normal distributions, indicating that the source of this variance has a strong, exponential effect on the resistance. We have demonstrated that tip-to-tip variance can be reduced by coating the tips with ethanethiol or butanethiol monolayers, or by performing the experiment under cyclohexane. These measures also have the effect of reducing the junction resistance. Contaminant layers of uncontrolled thickness may be the primary factor contributing to tip-to-tip variance in these experiments. Modification of tips with aliphatic monolayers replaces existing contaminants and increases the hydrophobicity of the tips. Similarly, the use of solvent removes contaminants and water from the surface of the tip. Reduction of the mean resistance values under these conditions could result because contaminant layers adsorbed to the tips are slightly thicker than

the monolayer and cyclohexane layers that are present between the tip and monolayer surface in the latter experiments.

Tips that were used to make many measurements showed a trend of increasing resistance with consecutive measurement, presumably because free or bound decanethiol molecules were removed from the surface, adhering to the tip over time. Junctions made with chemically modified tips and with unmodified tips under cyclohexane did not show this increase, but rather showed a slight decrease or no change in resistance. Adhesive forces in junctions made in air (adhesive forces under cyclohexane were small and not recorded) were observed to increase with or without chemical modification of the tips, probably indicating that in all cases, tips are plastically deformed, resulting in increasing contact areas. Increases in contact area would not be observed in the resistance for unmodified tip junctions, presumably because increases in contamination overshadowed this effect. The decrease in resistance for all other conditions may be explained in part by this increase in contact area, but may also be due to cleansing of the tip in solvent over time and degradation of the short-chain tip monolayer for the modified tip junctions. Both of these situations would result in a reduction of junction thickness and a stronger reduction in junction resistance than can be accounted for by an increase in contact area alone.

Sensitivity to contact area dependence requires very good control over those factors that influence variance in junction resistance. Even in experiments performed with C_4-modified tips, the tip-to-tip variance was too large to observe a decrease of resistance with increasing tip radius. The dependence of resistance on junction load skirts this variance because experiments can be performed with a single tip. Further exploration in conventional contact mechanics modeling of these junctions is currently underway.

Acknowledgment. C.D.F. thanks the NSF (DMR-0084404, CHE-0315165) for financial support. V.B.E. thanks the University of Minnesota Graduate School for financial assistance through the Doctoral Dissertation Fellowship.

References and Notes

(1) Engelkes, V. B.; Beebe, J. M.; Frisbie, C. D. *J. Am. Chem. Soc.* **2004**, *126*, 14287−14296.

(2) Kushmerick, J. G.; Lazorcik, J.; Patterson, C. H.; Shashidhar, R.; Seferos, D. S.; Bazan, G. C. *Nano Lett.* **2004**, *4*, 639−642.

(3) Lee, T.; Wang, W.; Klemic, J. F.; Zhang, J. J.; Su, J.; Reed, M. A. *J. Phys. Chem. B* **2004**, *108*, 8742−8750.

(4) Liu, B.; Bard, A. J.; Mirkin, M. V.; Creager, S. E. *J. Am. Chem. Soc.* **2004**, *126*, 1485−1492.

(5) Weiss, E. A.; Ahrens, M. J.; Sinks, L. E.; Gusev, A. V.; Ratner, M. A.; Wasielewski, M. R. *J. Am. Chem. Soc.* **2004**, *126*, 5577−5584.

(6) Kushmerick, J. G.; Naciri, J.; Yang, J. C.; Shashidhar, R. *Nano Lett.* **2003**, *3*, 897−900.

(7) Ramachandran, G. K.; Tomfohr, J. K.; Li, J.; Sankey, O. F.; Zarate, X.; Primak, A.; Terazono, Y.; Moore, T. A.; Moore, A. L.; Gust, D.; Nagahara, L. A.; Lindsay, S. M. *J. Phys. Chem. B* **2003**, *107*, 6162−6169.

(8) Salomon, A.; Cahen, D.; Lindsay, S.; Tomfohr, J.; Engelkes, V. B.; Frisbie, C. D. *Adv. Mater.* **2003**, *15*, 1881−1890.

(9) Wang, W.; Lee, T.; Reed, M. A. *Phys. Rev. B* **2003**, *68*, 035416/035411−035416/035417.

(10) Beebe, J. M.; Engelkes, V. B.; Miller, L. L.; Frisbie, C. D. *J. Am. Chem. Soc.* **2002**, *124*, 11268−11269.

(11) Chabinyc, M. L.; Chen, X.; Holmlin, R. E.; Jacobs, H.; Skulason, H.; Frisbie, C. D.; Mujica, V.; Ratner, M. A.; Rampi, M. A.; Whitesides, G. M. *J. Am. Chem. Soc.* **2002**, *124*, 11730−11736.

(12) Cui, X. D.; Zarate, X.; Tomfohr, J.; Sankey, O. F.; Primak, A.; Moore, A. L.; Moore, T. A.; Gust, D.; Harris, G.; Lindsay, S. M. *Nanotechnology* **2002**, *13*, 5−14.

(13) Cui, X. D.; Primak, A.; Zarate, X.; Tomfohr, J.; Sankey, O. F.; Moore, A. L.; Moore, T. A.; Gust, D.; Nagahara, L. A.; Lindsay, S. M. *J. Phys. Chem. B* **2002**, *106*, 8609−8614.

(14) Kushmerick, J. G.; Holt, D. B.; Yang, J. C.; Naciri, J.; Moore, M. H.; Shashidhar, R. *Phys. Rev. Lett.* **2002**, *89*, 086802/086801−086802/086804.

(15) Kushmerick, J. G.; Holt, D. B.; Pollack, S. K.; Ratner, M. A.; Yang, J. C.; Schull, T. L.; Naciri, J.; Moore, M. H.; Shashidhar, R. *J. Am. Chem. Soc.* **2002**, *124*, 10654−10655.

(16) Selzer, Y.; Salomon, A.; Cahen, D. *J. Am. Chem. Soc.* **2002**, *124*, 2886−2887.

(17) Selzer, Y.; Salomon, A.; Cahen, D. *J. Phys. Chem. B* **2002**, *106*, 10432−10439.

(18) Wold, D. J.; Haag, R.; Rampi, M. A.; Frisbie, C. D. *J. Phys. Chem. B* **2002**, *106*, 2813−2816.

(19) Chabinyc, M. L.; Chen, X.; Holmlin, R. E.; Jacobs, H. O.; Rampi, M. A.; Whitesides, G. M. *Abstr. Pap. − Am. Chem. Soc.* **2001**, *221st*, COLL-009.

(20) Cui, X. D.; Primak, A.; Zarate, X.; Tomfohr, J.; Sankey, O. F.; Moore, A. L.; Moore, T. A.; Gust, D.; Harris, G.; Lindsay, S. M. *Science* **2001**, *294*, 571−574.

(21) Holmlin, R. E.; Haag, R.; Chabinyc, M. L.; Ismagilov, R. F.; Cohen, A. E.; Terfort, A.; Rampi, M. A.; Whitesides, G. M. *J. Am. Chem. Soc.* **2001**, *123*, 5075−5085.

(22) Holmlin, R. E.; Ismagilov, R. F.; Haag, R.; Mujica, V.; Ratner, M. A.; Rampi, M. A.; Whitesides, G. M. *Angew. Chem., Int. Ed.* **2001**, *40*, 2316−2320.

(23) Wold, D. J.; Frisbie, C. D. *J. Am. Chem. Soc.* **2001**, *123*, 5549−5556.

(24) Hong, S.; Reifenberger, R.; Tian, W.; Datta, S.; Henderson, J.; Kubiak, C. P. *Superlattices Microstruct.* **2000**, *28*, 289−303.

(25) Wold, D. J.; Frisbie, C. D. *J. Am. Chem. Soc.* **2000**, *122*, 2970−2971.

(26) Bumm, L. A.; Arnold, J. J.; Dunbar, T. D.; Allara, D. L.; Weiss, P. S. *J. Phys. Chem. B* **1999**, *103*, 8122−8127.

(27) Slowinski, K.; Fong, H. K. Y.; Majda, M. *J. Am. Chem. Soc.* **1999**, *121*, 7257−7261.

(28) Slowinski, K.; Slowinska, K. U.; Majda, M. *J. Phys. Chem. B* **1999**, *103*, 8544−8551.

(29) Slowinski, K.; Chamberlain, R. V.; Miller, C. J.; Majda, M. *J. Am. Chem. Soc.* **1997**, *119*, 11910−11919.

(30) Bumm, L. A.; Arnold, J. J.; Cygan, M. T.; Dunbar, T. D.; Burgin, T. P.; Jones, L., II; Allara, D. L.; Tour, J. M.; Weiss, P. S. *Science* **1996**, *271*, 1705−1707.

(31) Slowinski, K.; Chamberlain, R. V., II; Bilewicz, R.; Majda, M. *J. Am. Chem. Soc.* **1996**, *118*, 4709−4710.

(32) Zhou, C.; Muller, C. J.; Deshpande, M. R.; Sleight, J. W.; Reed, M. A. *Appl. Phys. Lett.* **1995**, *67*, 1160−1162.

(33) Polymeropoulos, E. E.; Sagiv, J. *J. Chem. Phys.* **1978**, *69*, 1836−1847.

(34) Chernick, M. R. *Bootstrap Methods: A Practitioner's Guide*; Wiley: New York, 1999.

(35) Efron, B. *An Introduction to the Bootstrap*; Chapman & Hall: New York, 1993.

(36) Blackstock, J. J.; Li, Z.; Freeman, M. R.; Stewart, D. R. *Surf. Sci.* **2003**, *546*, 87−96.

(37) Levy, R.; Maalmoum, M. *Nanotechnology* **2002**, *13*, 33−37.

(38) Stark, R. W.; Drobek, T.; Heckl, W. M. *Ultramicroscopy* **2001**, *86*, 207−215.

(39) Beach, E. R.; Tormoen, G. W.; Drelich, J. *J. Adhes. Sci. Technol.* **2002**, *16*, 845−868.

(40) Burnham, N. A.; Dominguez, D. D.; Mowery, R. L.; Colton, R. J. *Phys. Rev. Lett.* **1990**, *64*, 1931−1934.

(41) Yourdshahyan, Y.; Zhang, H. K.; Rappe, A. M. *Phys. Rev. B* **2001**, *63*, 081405/081401−081405/081404.

(42) Cappella, B.; Dietler, G. *Surf. Sci. Rep.* **1999**, *34*, 1−104.